

Quantifying Local and Cooperative Components in the Ferroelectric Distortion of BaTiO₃: Learning from the Off-Center Motion in the MnCl₆⁵⁻ Complex Formed in KCl:Mn⁺

J. M. García-Lastra,^{*,†} P. García-Fernández,[‡] F. Calle-Vallejo,[§] A. Trueba,[‡] J. A. Aramburu,[‡] and M. Moreno[‡]

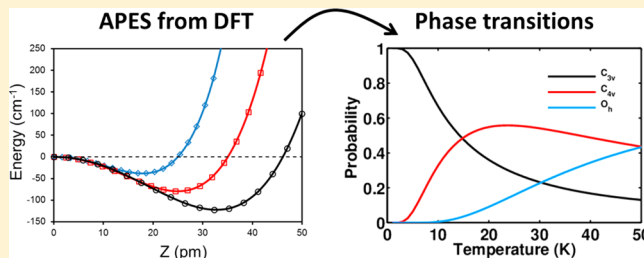
[†]Department of Energy Conversion and Storage, Technical University of Denmark, DK-4000 Roskilde, Denmark

[‡]Departamento de Ciencias de la Tierra y Física de la Materia Condensada, Universidad de Cantabria, Avenida de los Castros s/n, 39005 Santander, Spain

[§]Laboratoire de Chimie, Institut de Chimie, Université de Lyon, CNRS, Ecole Normale Supérieure de Lyon, 46 Allée d'Italie, 69364 Lyon Cedex 07, France

Supporting Information

ABSTRACT: The delicate balance between cooperative and local contributions in the ferroelectric distortions of BaTiO₃ is explored by means of ab initio calculations. As a salient feature, it is found that a *single* Ti⁴⁺ ion in BaTiO₃ is not allowed to move off-center at ambient pressure, while this is no longer true if the lattice is expanded by only ~5%, stressing the high sensitivity of the local contribution to chemical and hydrostatic pressures. In order to further understand the effect of local contributions on the phase transition mechanism of ferroelectrics, we have investigated the surprising C_{3v} → C_{4v} → O_h local transformations occurring in the 10–50 K temperature range for the MnCl₆⁵⁻ complex formed in KCl:Mn⁺ that mimic the behavior of BaTiO₃. From Boltzmann analysis of the vibronic levels derived from ab initio calculations and considering decoherence introduced by random strains, the present calculations reproduce the experimental phase sequence and transition temperatures. Furthermore, our calculations show that the off-center instability in KCl:Mn⁺ would be suppressed by reducing by only 1% the lattice parameter, a situation that then becomes comparable to that found for BaTiO₃ at ambient pressure. The present results thus stress the deep link between the structural phase transitions of ferroelectric materials and local phase transitions displayed by transition-metal impurities in insulators.



1. INTRODUCTION

Materials with ferroelectric properties have been intensively researched for their many applications, such as transducers, actuators, capacitors, and memories.^{1–6} Among the most in-depth-investigated ferroelectric materials, BaTiO₃ is of particular interest primarily because of its simple perovskite structure, containing TiO₆⁸⁻ complexes, and its typical three first-order phase transitions of cubic (C phase, $T > 393$ K) → tetragonal (T phase, 393 K $> T > 278$ K) → orthorhombic (O phase, 278 K $> T > 183$ K) → rhombohedral (R phase, $T < 183$ K). BaTiO₃ was the first ferroelectric oxide, and even 60 years after its discovery, it is the most widely used ferroelectric material⁴ and the most important multilayer ceramic dielectric.³ Moreover, intense experimental efforts targeted toward the synthesis of ferroelectric nanostructures based on BaTiO₃ can be expected to further expand its applicability^{5–7} including the development of ultracapacitor power systems to replace electrochemical batteries.⁸

Despite the huge amount of experimental and theoretical work carried out on this material during the past 6 decades, there are, however, basic aspects that are still not well

understood and controversial, starting with the microscopic origin of ferroelectric distortions. In that respect, while there is a consensus that the occurrence of ferroelectricity in oxoperovskites is a subtle phenomenon that depends on a delicate competition between local forces and cooperative long-range effects, there are, however, different points of view on the role of both contributions.^{9,10}

The first microscopic model of the ferroelectric distortion was developed in 1950 by Slater.¹¹ In his seminal work, Slater assumed that the ferroelectric behavior of BaTiO₃ should be caused by cooperative long-range dipolar forces that tend to destabilize the high-symmetry configuration of Ti⁴⁺ ions favored by localized elastic forces opposing the off-center displacements.^{9,10} In Slater's model, the off-center displacement of Ti⁴⁺ ions from the center of TiO₆⁸⁻ octahedra due to long-range dipolar effects is the unique driving force for the appearance of ferroelectricity, *assuming* the rest of the ions in the lattice are fixed.¹¹ Later on, Cochran developed a more

Received: December 10, 2013

Published: June 19, 2014

sophisticated model involving the dynamics of all lattice ions, introducing the soft-mode concept and theory for displacive phase transitions,^{12,13} considering that all Ti^{4+} ions stay at the center of the oxygen octahedron in the C phase but will displace collectively along the $\langle 001 \rangle$, $\langle 011 \rangle$, and $\langle 111 \rangle$ polarization directions for the T, O, and R phases, respectively. This model was supported by experimental data concerning the temperature-dependent properties of the soft mode¹ and was later quantified by ab initio calculations,¹⁴ making Cochran's model very popular in the field. More recently and connected to this subject, there has been strong interest¹⁵ in the minimum (critical) thickness that allows a ferroelectric material thin film to display spontaneous polarization. The strong influence of long-range terms necessarily implies that this thickness must be finite, imposing restrictions on the development of ferroelectric-based electronics.^{15,16}

However, X-ray experiments performed by Comes et al.¹⁷ and Chaves et al.¹⁸ showed that the presence of diffuse scatterings in all except the R phase also suggests a spontaneous symmetry breaking and short-range ordering of local structures, which are inconsistent with the displacive model. Moreover, this model contradicts many other experimental results, for example, X-ray absorption fine structure,¹⁹ electron paramagnetic resonance (EPR),²⁰ and nuclear magnetic resonance²¹ data, which show that the local structural environment remains *approximately rhombohedrally* distorted in all phases. Also, ab initio calculations have clearly shown that short-range Ti–O covalent hybridization is essential to the softening of the ferroelectric mode producing the instability.²² This idea, strongly connected with the pseudo-Jahn–Teller model previously developed by Bersuker^{23–25} for the ferroelectric instability in the TiO_6^{8-} complexes, proposes that the primary driving force for the off-center $\langle 111 \rangle$ displacements of Ti^{4+} ions is the vibronic coupling of the ground state with appropriate excited states via a local vibrational mode of the TiO_6^{8-} complex, producing a reinforcement of the covalent bonding between Ti^{4+} and three of the six O^{2-} anions.

It is worth noting now that a situation similar to that of ferroelectric materials occurs in a number of impurity centers in solids.²⁶ These centers present a spontaneous off-center motion that breaks the symmetry of the crystal, creating an electric dipole that can be oriented and stabilized in different directions by the application of electric fields. In these model systems, *only* a local component is present, namely, a change in the bonding pattern that favors the displacements, in contrast to what is believed to happen in ferroelectric materials.^{26–28}

At this point, a question arises: would it be possible that in some ferroelectrics, under certain conditions, the local components also favor ferroelectricity reducing, for example, the critical thickness? Experimental techniques can help to give a glimpse into the role of local and long-range contributions in the phase transitions of ferroelectrics.^{29,30} Nevertheless, it is still not possible to quantify and separate accurately both effects solely from experiments, answering the question above. However, this aim can be realized through theoretical models based on ab initio calculations. In particular, Vanderbilt et al. obtained a remarkably good agreement between the theoretical and experimental phase-transition temperatures for BaTiO_3 ^{31,32} by decomposing the interactions in the crystal in short- and long-range terms.

In order to explore in more detail the relationship between ferroelectric distortions and off-center instabilities in impurities, it should be noted that some of the latter change their average

displacement orientation at critical temperatures, analogous to the phase transitions in ferroelectrics. For this reason, some authors christened this temperature-dependent orientation in impurity centers as local phase transitions (LPTs)^{33,34} One of the clearest examples of LPTs takes place in KCl doped with the *unusual* Mn^+ ion ($3d^5 4s^1$ electron configuration), which enters the KCl lattice replacing K^+ ions.³⁵ Here, the temperature dependence of the EPR spectra measured by Badalyan et al. gives evidence of two LPTs showing *some similarity* to the ferroelectric phase transitions that occur in BaTiO_3 .³⁵ Indeed, in $\text{KCl}:\text{Mn}^+$, three different EPR spectra were measured in the temperature range 4–50 K, with *reversible* transitions among them. Above ~ 40 K, the spectrum is isotropic, corresponding with a cubic O_h symmetry and virtually temperature-independent. Locally, this resembles the cubic phase of BaTiO_3 above 403 K. In the temperature range 40–20 K, the EPR signal of the $\text{KCl}:\text{Mn}^+$ cubic center decreases to zero, while a new signal corresponding to a slightly anisotropic center with tetragonal C_{4v} symmetry grows. This is analogous to the observed BaTiO_3 tetragonal phase between 278 and 403 K. Below 14 K, Badalyan et al. detected a third anisotropic spectrum in $\text{KCl}:\text{Mn}^+$ with trigonal C_{3v} symmetry that looks like the rhombohedral phase of BaTiO_3 below 183 K. The only phase of BaTiO_3 that does not have a local analogue in $\text{KCl}:\text{Mn}^+$ is the orthorhombic one between 183 and 278 K. Because of the similarities between LPTs in $\text{KCl}:\text{Mn}^+$ and phase transitions in BaTiO_3 , the study of $\text{KCl}:\text{Mn}^+$ can *also* give insight into systems that are ferroelectric and magnetic (multiferroics), where both effects originate on the *same* ion, in contrast with typical materials of this kind like BiFeO_3 . It is worth noting that the EPR technique is particularly appropriate to study LPTs at *low* temperatures because an increase of the temperature, T , usually favors the broadening of the signals. For this reason, the LPTs of $\text{BaF}_2:\text{Mn}^{2+}$ ^{35–37} or $\text{CuCl}_4(\text{H}_2\text{O})^{2-}$ complexes in NH_4Cl ^{38–40} undoubtedly observed by EPR take place at $T < 50$ K.

Bearing these facts in mind, this work is addressed to *quantify* the role of local and cooperative contributions in BaTiO_3 and, in general, in ferroelectric distortions from a new chemical perspective using ab initio calculations. For clearing up this relevant matter, local and cooperative contributions in BaTiO_3 are obtained by means of a practical approach based on ab initio calculations performed on *supercells* of different sizes. At the same time, the surprising $C_{3v} \rightarrow C_{4v}$ and $C_{4v} \rightarrow O_h$ symmetry changes observed for MnCl_6^{5-} complexes formed in $\text{KCl}:\text{Mn}^+$,³³ driven *only* by the local contribution, are explored in detail. To the authors' knowledge, this is the first time that a system with *several* LPTs has been studied theoretically by means of ab initio calculations.

As a salient feature, it will be shown that the local component is very sensitive to hydrostatic and chemical pressures, a fact that makes it possible to conciliate the results on the BaTiO_3 and MnCl_6^{5-} complexes in $\text{KCl}:\text{Mn}^+$. Indeed, it will be seen that a *single* Ti^{4+} ion in BaTiO_3 moves off-center after *only* a 5% lattice expansion, while the off-center instability in $\text{KCl}:\text{Mn}^+$ is suppressed by reducing 1% the host lattice parameter.

This paper is arranged as follows. The employed calculation methods are described in the next section, while the main results obtained in the present work are discussed in the following one. A summary of the main conclusions reached in this work is reported in the last section.

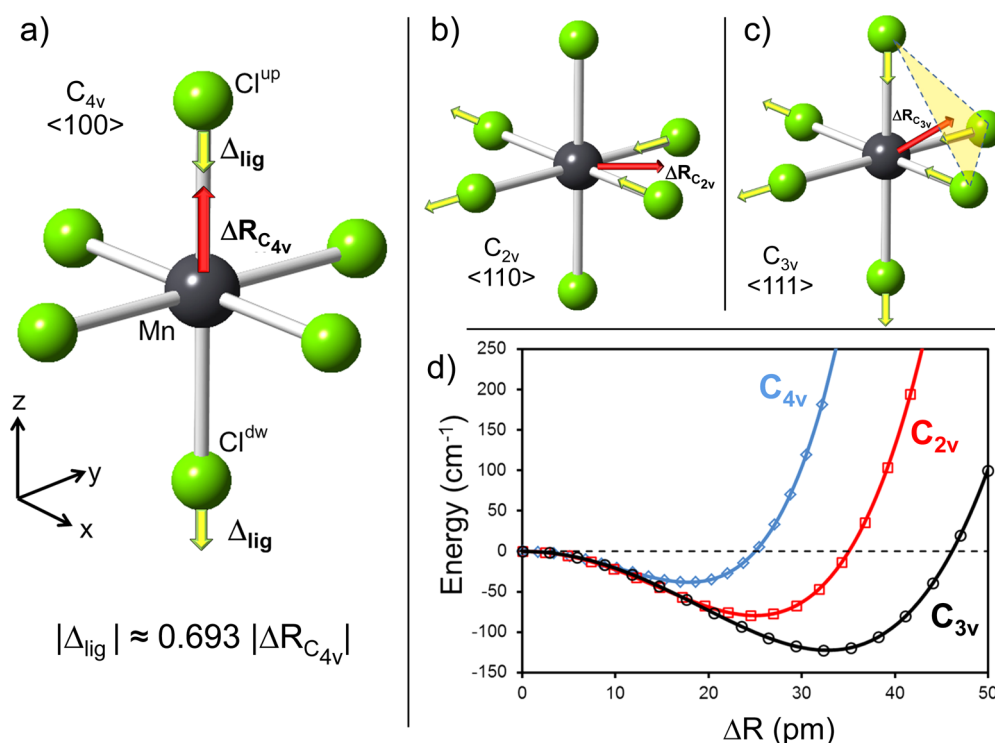


Figure 1. (a) Tetragonal C_{4v} off-center distortion along a $\langle 100 \rangle$ direction in the MnCl_6^{5-} complex formed in $\text{KCl}:\text{Mn}^+$. The distortion shown corresponds exactly with the t_{1u} normal vibrational mode in the z direction. The normal coordinate of the mode is $Q_z = \{1/[1 + 2(\Delta_{\text{lig}})^2]^{1/2}\}(\Delta R_{C_{4v}} \cdot \text{Mn}_z - \Delta_{\text{lig}} \cdot [\text{Cl}_z^{\text{up}} + \text{Cl}_z^{\text{dw}}])$, where Mn_z , Cl_z^{up} , and Cl_z^{dw} are the unit vectors of displacement in the z direction for Mn, Cl^{up} , and Cl^{dw} ions, respectively. (b) The same for the orthorhombic C_{2v} off-center distortion along a $\langle 110 \rangle$ direction. (c) The same for the trigonal C_{3v} off-center distortion along a $\langle 111 \rangle$ direction. (d) Calculated stabilization energies of the MnCl_6^{5-} complex in $\text{KCl}:\text{Mn}^+$ upon off-center displacements of Mn^+ ions in the $\langle 100 \rangle$, $\langle 110 \rangle$, and $\langle 111 \rangle$ directions. Although the energy is plotted versus Mn displacements, the concomitant Cl displacements are also included in the calculations.

2. COMPUTATIONAL METHODOLOGY

The off-center motion of Mn^+ ions in $\text{KCl}:\text{Mn}^+$ has been studied in the realm of the density functional theory (DFT) through *periodic* calculations performed by means of the *PWSCF* code.⁴¹ We chose the local density approximation (LDA)⁴² to treat the exchange-correlation energy because it has been shown that this type of functional provides an accurate description of the energy barriers in ferroelectric materials.^{22,31,32} Periodic calculations have been performed by means of a $3 \times 3 \times 3$ supercell (216 atoms) in which a K^+ ion of the KCl lattice is replaced by a Mn^+ ion. The k -point grid is reduced to just the Γ point. The occupation of the one-electron states has been calculated at an electronic temperature of $k_B T = 0.01$ eV. In all calculations, the ion cores are replaced by norm-conserving pseudopotentials from the Fritz–Haber Institute library.⁴³ The kinetic energy cutoff is taken at 50 hartree. Only the positions of the Mn^+ ion and its first two shells of neighbors along the $\langle 100 \rangle$ direction (involving six Cl^- ions in the first shell and six K^+ ions in the second shell) have been optimized in the present calculations. The positions of the rest of ions are kept frozen at their experimental values.^{44,45}

For the study of BaTiO_3 , we have performed again periodic calculations in the DFT framework using the LDA functional. As a salient feature, we have employed two different supercells, namely, a $1 \times 1 \times 1$ supercell (five atoms) and a $3 \times 3 \times 3$ supercell (125 atoms). The k -point grid size was $3 \times 3 \times 3$ for the former, whereas for the latter, it was just reduced to the Γ point. The rest of the calculation parameters were the same as those in the $\text{KCl}:\text{Mn}^+$ study.

In order to have information for finite temperatures and simulate the LPTs observed in $\text{KCl}:\text{Mn}^+$, it is necessary to calculate the free energy, requiring knowledge of the vibrational levels associated with the energy surface of the electronic ground state and their change in occupation with temperature. For obtaining the vibrational wave functions, $\chi(Q)$, and their corresponding energies from eq 1, we have

used the *VibE* code,³⁷ where each $\chi(Q)$ is expanded in a large number of Gaussian functions in each dimension (35^3 gaussians in total), whose exponents are optimized. See the Supporting Information for more details on these calculations.

3. RESULTS AND DISCUSSION

3.1. Geometry Optimizations and Off-Center Distortions in $\text{KCl}:\text{Mn}^+$. In the first step, we have imposed a cubic O_h symmetry to the system, thus keeping the on-center position of the Mn^+ ion. Under such a restriction, the distance from Mn^+ to its six Cl^- ligands is found to be $R_0 = 3.15$ Å, a value that is *practically identical* to that of the $\text{K}^+ - \text{Cl}^-$ distance in pure KCl. This shows that K^+ and Mn^+ ions have similar ionic radii, ruling out once more size effects being responsible for the off-center displacements of impurities in insulators.^{26–28}

In the second step, we have calculated the off-center displacement of the Mn^+ ion, ΔR_i , and the stabilization energy with respect to the cubic symmetry, ΔE_i , considering three possible lower symmetries, namely, tetragonal C_{4v} , orthorhombic C_{2v} , and trigonal C_{3v} , which correspond to motion along the $\langle 100 \rangle$, $\langle 110 \rangle$, and $\langle 111 \rangle$ directions, respectively. The most stable configuration is found in the trigonal C_{3v} symmetry, with $\Delta E_{\text{trig}} = -118$ cm⁻¹ and $\Delta R_{\text{trig}} = 31$ pm $\ll R_0$ (Figure 1). Both the very low stabilization energy and the direction of the off-center displacement are in accordance with the EPR results from Badalyan et al.³³ For tetragonal and orthorhombic off-center symmetries, we have obtained, respectively, $\Delta E_{\text{tet}} = -38$ cm⁻¹ and $\Delta E_{\text{orth}} = -80$ cm⁻¹ for the stabilization energies and $\Delta R_{\text{tet}} = 18$ pm and $\Delta R_{\text{orth}} = 25$ pm for the off-center displacements. It is worth noting that $\Delta R_{\text{tet}} \approx \Delta R_{\text{orth}}/\sqrt{2} \approx$

$\Delta R_{\text{trig}}/\sqrt{3}$ and $\Delta E_{\text{tet}} \approx \Delta E_{\text{orth}}/2 \approx \Delta E_{\text{trig}}/3$. These ratios support the off-center motion being due to the vibronic coupling of the ground state with certain excited states through the t_{1u} modes of the MnCl_6^{5-} complex.^{26,37,45} Each of the three t_{1u} vibrational modes, which are degenerate under O_h symmetry, consist basically of an off-center displacement of the Mn^+ ion along one of the three equivalent $\langle 100 \rangle$ directions, accompanied by an approach of the closest Cl^- ion toward the Mn^+ ion and a separation from the furthest Cl^- ion (i.e., an antistretching t_{1u} mode; see Figure 1a–c).⁴⁵ Thus, the orthorhombic C_{2v} and trigonal C_{3v} distortions can simply be seen as the sum of two (for C_{2v}) or three (for C_{3v}) independent components of the C_{4v} distortion. In spite of the differences in the electronic state, this result is in striking agreement with the pseudo-Jahn–Teller model for the off-center Ti^{4+} displacement in BaTiO_3 (see eq 4.100 in ref 24), where the addition of three independent orbital–orbital couplings produces the final distortion along $\langle 111 \rangle$. As a salient feature, we have also made calculations fixing all atomic positions except the Mn^+ one, and under this constraint, no off-center displacement is stabilized in any direction. These results thus emphasize that the *simultaneous* motion of Cl^- ligands as described by the lowest t_{1u} mode is crucial for having an off-center displacement of the Mn^+ impurity in KCl. In this respect, the fact that the off-center motion of the Mn^+ ion alone is not favorable further reinforces the idea that the off-center motion is not controlled by the size of the metal ion inside the octahedral cage created by the ligands. Moreover, in calculations performed using a lattice parameter, a , reduced *only* by 1% with respect to the experimental value, $a = 315$ pm, the off-center instability disappears, stressing that, in general, pressure acts against the occurrence of off-center phenomena.^{26–28} This behavior has been experimentally observed for $\text{SrF}_2:\text{Cu}^{2+}$.⁴⁶

3.2. Chemical Bonding and Off-Center Instability in $\text{KCl}:\text{Mn}^+$. Once the structure of the complex is established, we study the origin of the distortion. Like in the case of Fe^+ impurities in SrCl_2 ,²⁸ we find that the distortion is sensitive to the change of the electronic state in the manganese impurity. This fact underlines that changes in the chemical bonding accompanying the distortion, described by the so-called pseudo-Jahn–Teller mechanism,^{24,26} play a key role for understanding the off-center instability. In this sense, we have verified that calculations for the Mn^{2+} impurity ($3d^5$ configuration) in KCl yield no off-center distortion at all, at variance with what is found for the less common Mn^+ cation ($3d^5 4s^1$ electron configuration) in the same lattice. Because the main difference in the electronic configuration between Mn^{2+} and Mn^+ is the occupancy of the mainly $4s(\text{Mn})$ orbital, we expect this orbital to play a key role in the distortion. Our calculations indicate that at the high-symmetry configuration the electron spends 56% of the time on the $4s(\text{Mn})$ orbital and 44% on the Cl^- ligands, and this proportion remains almost constant upon moving to the other, lower-symmetry, minima. The main change in the electron distribution is found to come from hybridization of the $4s(\text{Mn})$ orbital with $4p(\text{Mn})$ when the system is distorted through a pseudo-Jahn–Teller mechanism.²⁴ We have verified that, in the trigonal C_{3v} phase, the $4s(\text{Mn})$ orbital hybridizes with the $4p_i(\text{Mn})$ ones ($i = x, y, z$), with the contribution to the valence band wave function from the Mn^+ ion being $0.958[4s(\text{Mn})] + 0.014[4p_x(\text{Mn})] + 0.014[4p_y(\text{Mn})] + 0.014[4p_z(\text{Mn})]$. The magnitude of hybridization with $4p$ levels ($\sim 1\%$) in the present case is consistent with that found for $\text{SrCl}_2:\text{Fe}^+$ ($\sim 4\%$), taking into account that

the equilibrium distortion in $\text{KCl}:\text{Mn}^+$, 0.31 \AA , is substantially smaller than the huge $\langle 001 \rangle$ off-center motion in $\text{SrCl}_2:\text{Fe}^+$ (1.3 \AA).²⁸ Thus, this result underlines the importance of knowing the associated changes in chemical bonding for understanding the occurrence of an off-center instability. According to this, the off-center instability of an impurity ion in an insulating lattice can hardly be understood considering that ions are rigid and the ion size is the only driving force. Indeed, for $\text{KCl}:\text{Mn}^+$, the results shown in section 3.1 indicate that the impurity and host cation have similar ionic radii ($\sim 1.30 \text{ \AA}$), and thus it is not easy to explain the off-center instability of Mn^+ ions in KCl *only* on the basis of the ion size. Furthermore, the present calculations indicate that the *smaller* Mn^{2+} ion (ionic radius 0.80 \AA) does not go off-center in KCl in good agreement with experimental data.^{47,48} This view is also supported by other relevant experimental facts. So, among the d^9 impurities placed in CaF_2 , only Ni^+ , which is the biggest one (ionic radius of 0.9 \AA),⁴⁹ moves drastically off-center, while the smaller Cu^{2+} and Ag^{2+} cations remain on-center.²⁶ Along this line, in a $\text{Ge}_{0.9}\text{Pb}_{0.1}\text{Te}$ solid solution, extended X-ray absorption fine structure data prove that the *large* Pb^{2+} ion moves significantly off-center.⁵⁰ Similarly, the tilting instability observed for some KMf_3 perovskites ($M = 3d^n$ ion) has been shown to be greatly influenced by the population of the t_{2g} subshell rather than by the size of the ions.⁵¹

3.3. Ab Initio Vibronic Model for the LPTs in $\text{KCl}:\text{Mn}^+$.

Even though we know that the global energy minima of the $\text{KCl}:\text{Mn}^+$ system are located in the *eight equivalent* $\langle 111 \rangle$ off-center displacements, in order to properly understand the LPTs observed by Badalyan et al.,³⁵ it is fully necessary to study the adiabatic potential energy surface (APES) and obtain the nuclear wave functions and associated energy levels. To achieve this goal, we have used an adiabatic model, decoupling the nuclear wave functions from the electronic ones, in which the calculated numerical APES for the electronic ground state was fitted to the following energy expression, $E(Q)$, depending only on the normal coordinates Q_i ($i = x, y, z$) of the t_{1u} vibrational mode of the MnCl_6^{5-} complex:

$$E(Q) \approx E_{\text{oct}} + \frac{1}{2}K(Q_x^2 + Q_y^2 + Q_z^2) + \frac{1}{4}G(Q_x^4 + Q_y^4 + Q_z^4) + H(Q_x^2Q_y^2 + Q_x^2Q_z^2 + Q_z^2Q_y^2) \quad (1)$$

In this expression, the total force constant, K , has to be negative if an off-center instability takes place. It should be recalled here that for a complex like MnCl_6^{5-} the vibronic mixing of the electronic ground state with excited states always provides a *negative* contribution, termed K_v , to the total force constant K .^{24,26} This contribution, directly reflecting the change of the electronic density associated with the distortion, acts against another one, termed K_0 , which is positive²⁴ and related only to the electronic density at the *undistorted* position. This local mechanism thus explains the existence of an off-center instability in an impurity, where long-range effects are absent, provided $|K_v| > K_0$, a condition first stressed by Bersuker.²⁴ Model impurity systems where the vibronic mechanism has been proven to be responsible for the structural instability are discussed in refs 27, 28, 37, and 40. The present reasoning explains, at least qualitatively, why for a given impurity placed in different isomorphous lattices a structural instability is favored by lattices with small force constants.²⁶ Indeed, in such

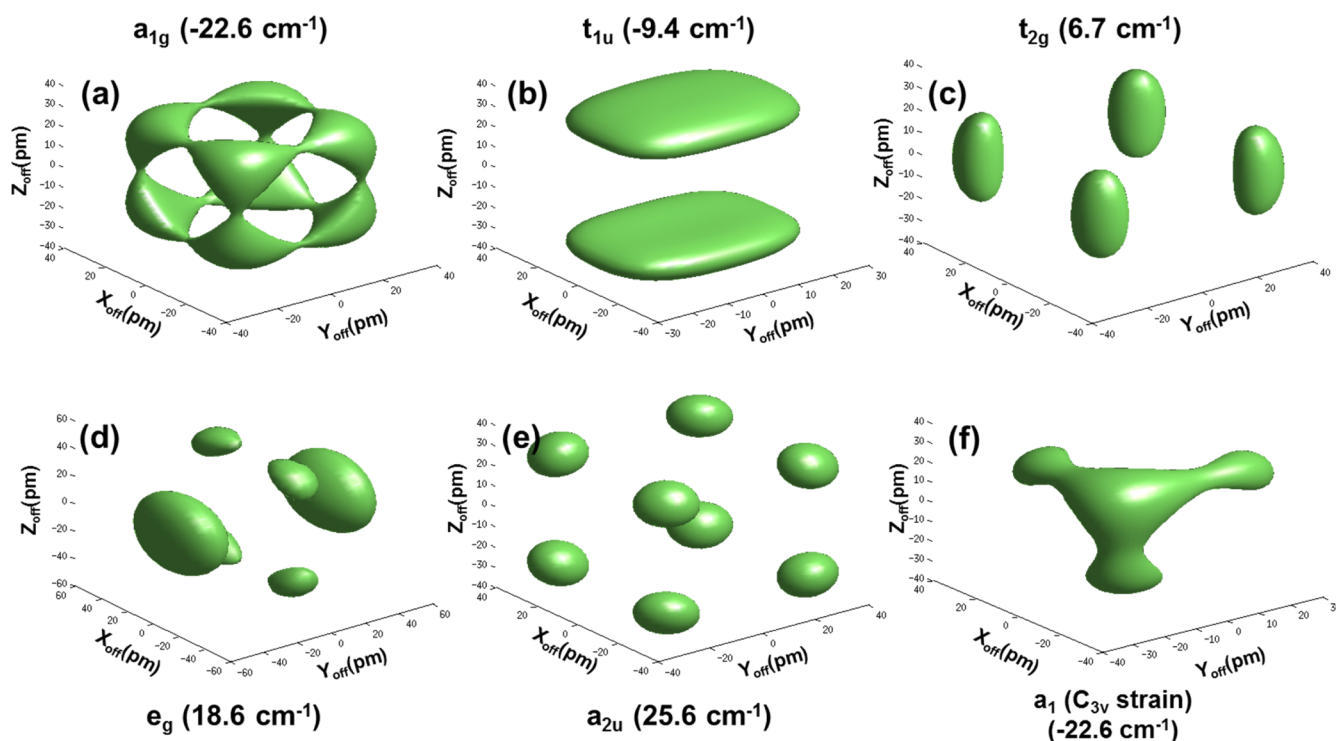


Figure 2. (a–e) Calculated energies (in cm^{-1}) and probability densities for the five lowest vibronic states corresponding to the APES of eq 1 along the unstable off-center vibrational modes of KCl:Mn^{2+} when no strain is present. For t_{1u} , t_{2g} , and e_g degenerate states, only one of them is plotted. (f) a_{1g} ground state when a strain described by $S = 3 \times 10^{-2} \text{ cm}^{-1}/\text{pm}$ is applied along the $[111]$ direction (see the text for details).

cases, it is easier that the vibronic admixture of the ground with excited states, involving the vibronic K_v contribution, can lead to $K < 0$. This explains why Mn^{2+} and Cu^{2+} impurities in NaCl do not move off-center like those in the KCl host lattice^{26,35} or why the Ag^{2+} cation moves off-center only in the softer SrCl_2 lattice but not in the CaF_2 and SrF_2 crystals.²⁶ Similarly, the local symmetry around a Mn^{2+} impurity in CaF_2 and SrF_2 is cubic but only tetrahedral in BaF_2 .^{37,53} The importance of low force constants for observing vibronic instabilities is also well clarified in the study on $\text{CuCl}_4\text{X}^{2-}$ complexes ($X = \text{H}_2\text{O}, \text{NH}_3$) in NH_4Cl .⁴⁰

In order to have information for finite temperatures and simulate the LPTs observed in KCl:Mn^{2+} , we have calculated the nuclear densities of the vibrational states employing the method described in the Computational Methodology section and the Hamiltonian in eq 1. The calculated nuclear densities for the lowest energy levels are shown in Figure 2. Of these wave functions, the ground state (a_{1g}) and the fourth excited state (a_{2u}) have cubic symmetry, while the wave functions of the first (t_{1u}), second (t_{2g}), and third (e_g) excited states display tetragonal symmetry (see the Supporting Information for more details on the origin of these levels).

A central question in this analysis is to know the mean Mn^{2+} off-center displacements along the x , y , and z directions, termed $\langle X_{\text{off}} \rangle$, $\langle Y_{\text{off}} \rangle$, and $\langle Z_{\text{off}} \rangle$, respectively. If the symmetry of the full Hamiltonian is perfectly cubic, the condition $\langle X_{\text{off}} \rangle = \langle Y_{\text{off}} \rangle = \langle Z_{\text{off}} \rangle = 0$ is, of course, fulfilled by all $\chi(Q)$ wave functions, just reflecting that the system can be found in one of the eight C_{3v} minima with the same probability. Thus, if the symmetry is strictly cubic, the coherent a_{1g} wave function would give rise at $T = 0 \text{ K}$ to an EPR spectrum displaying cubic rather than C_{3v} symmetry. A situation similar to this one is found in the dynamic Jahn–Teller effect observed in a few systems such as

MgO:Cu^{2+} .^{24,54–57} However, random strains, which are present in every real crystal,^{37,55,56,58,59} break the coherence in the $\chi(Q)$ wave functions and tend to localize solutions, thus favoring the detection of a lower symmetry. Evidently, this localization will be opposed by tunneling among the eight wells, the phenomenon responsible for the energy splitting of the a_{1g} , t_{1u} , t_{2g} , and a_{2u} levels in Figure 2. According to these facts, we have included in our model the influence of a random strain field on the electronic ground state, adding to the APES of eq 1 a term with the form

$$V_{\text{strain}}(Q) \approx S(\gamma_x Q_x + \gamma_y Q_y + \gamma_z Q_z) \quad (2)$$

Here, γ_i ($i = x, y, z$) means the cosine directors, while the S parameter reflects the coupling between the electronic ground state and strain field. As a salient feature, we have found that very low values of S break the coherence in the a_{1g} ground state and favor the localization, as shown on Figure 2f. More precisely, we have found that if $V_{\text{strain}}(Q)$ makes the well along the $\langle 111 \rangle$ direction only 1 cm^{-1} more stable than that along $\langle -1-1-1 \rangle$ (corresponding to $S = 3.5 \times 10^{-4} \text{ eV/\AA}$ and $\gamma_x = \gamma_y = \gamma_z$), then the average displacement of the Mn^{2+} ion, $\langle \Delta R \rangle$, is already equal to 26 pm and the local symmetry around Mn^{2+} is trigonal. However, this sensitivity is not the same for strains in all directions, and we have verified that the a_{1g} ground state is more strongly influenced by trigonal strain fields than for those that are tetragonal ($\gamma_x = \gamma_y = 0; \gamma_z = 1$). A different situation is, however, found for excited t_{1u} and t_{2g} vibronic levels, which are clearly more sensitive to a tetragonal than to a trigonal strain field. For instance, under a tetragonal strain field with $S = 3.5 \times 10^{-4} \text{ eV/\AA}$, a value of $\langle \Delta R \rangle = 17 \text{ pm}$ is found for t_{1u} , while this figure becomes 45% smaller for a trigonal strain field. A similar situation holds for t_{2g} states. With regard to the a_{2u} , e_g , and higher excited vibronic states, they have been found to be

practically insensitive to the strain field because of the dominance of tunneling and kinetic energy over the potential creating the interwell barriers described by eq 1, yielding a local symmetry that can be considered cubic ($\langle\Delta R\rangle \approx 0$ pm). This situation is similar to that of hydrogen-bonded N_2H_7^+ ions,⁶⁰ where the energy surface of the proton shows a double well but experimentally the system is only observed for the transition-state geometry displaying a higher potential energy.

Owing to these relevant facts, we have assumed that when the system is placed in the a_{1g} ground state, the random strain field favors the observation of C_{3v} symmetry. By contrast, if the system is placed in t_{1u} and t_{2g} states, it would display C_{4v} symmetry because random strain will favor observation of the system in this configuration, while the local symmetry would be cubic for a_{2u} and e_g and also higher vibronic states. This situation is thus similar to that found in $\text{BaF}_2:\text{Mn}^{2+}$, where the vibronic ground state displays T_d symmetry while all excited states lead to O_h symmetry.³⁷ The population of excited states upon increasing temperature allows one to understand the $T_d \rightarrow O_h$ LPT at $T \approx 45$ K in $\text{BaF}_2:\text{Mn}^{2+}$. Similarly, the break of coherence in Jahn–Teller systems of Cu^{2+} with 6-fold coordination is ascribed to tetragonal random strains.^{55,56,58}

Therefore, it is now crucial to explore whether the different LPTs observed by EPR in $\text{KCl}:\text{Mn}^{+33}$ can reasonably be accounted for on the same grounds. From the energies of the vibronic levels (Figure 2), it is straightforward to calculate their relative populations at a given temperature, and thus the probability of observing the system in a particular symmetry, P_i . Reducing our span of states to those shown in Figure 2, we can write the probabilities for each symmetry as $P_{C_{3v}} = P_{a_{1g}}$, $P_{C_{4v}} = P_{t_{1u}} + P_{t_{2g}}$, and $P_{O_h} = P_{a_{2u}}$. It should be noted that there are no states leading to C_{2v} symmetry (which is observed in BaTiO_3 but not in $\text{KCl}:\text{Mn}^+$) because the action of random strains over different vibrational levels favors the observation of either trigonal or tetragonal symmetries. Figure 3 shows the

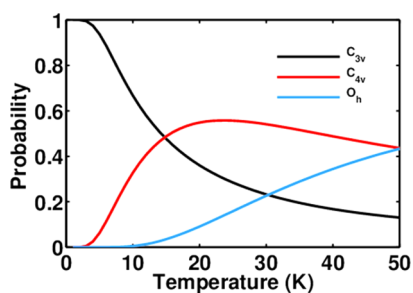


Figure 3. Calculated probabilities of each of the local phases in $\text{KCl}:\text{Mn}^+$ as a function of the temperature.

dependence of the different P_i upon T . We can see that below 15 K our model predicts that C_{3v} symmetry is the most probable one, while C_{4v} dominates in the range 15–50 K and O_h is the preferred one above 50 K. These results are thus in remarkably good agreement with Badalyan et al. experiments,³³ where LPTs occurred at 14 and 40 K. Moreover, they support that the local $C_{3v} \rightarrow C_{4v}$ and $C_{4v} \rightarrow O_h$ symmetry changes observed for MnCl_6^{5-} in KCl can be understood just considering the ground and first vibrational states emerging from the eight equivalent minima, together with the effects of unavoidable random strains. These results thus underline the relationship between LPTs for MnCl_6^{5-} in KCl and the ferroelectric phase transitions.

3.4. Quantifying Local and Cooperative Contributions to the Off-Center Distortions in BaTiO_3 . Let us now analyze the Ti^{4+} off-center displacements in BaTiO_3 combining Slater's model for ferroelectricity with DFT calculations. Within Slater's model, only the Ti^{4+} ion is allowed to move from its location, while the rest of the ions are fixed at their corresponding positions in a perfect cubic perovskite structure.¹¹ Although this model does not fully reflect the complexity of phase transitions in BaTiO_3 , which involve all ions in the lattice,^{9,12,32} it, however, allows us to separate the local and cooperative contributions to the off-center displacement's stabilization in a straightforward manner.

To achieve this goal, we have calculated the energies along the $\langle 100 \rangle$, $\langle 110 \rangle$, and $\langle 111 \rangle$ off-center displacements of the Ti^{4+} ion in two steps. In the first step, we have performed a DFT calculation using the simple unit cell with five atoms of BaTiO_3 in its cubic phase. Because of the periodic boundary conditions of the calculation, Ti^{4+} ion displacements take place in every cell of the crystal, and thus we observe both local and cooperative contributions all together. In a second step, we repeat the same calculations but use a $3 \times 3 \times 3$ supercell (125 atoms) instead of a $1 \times 1 \times 1$ one. In this case, we have 27 Ti^{4+} ions, but only one of them is allowed to move. In this way, we isolate the local contributions to the off-center displacements in the $\langle 100 \rangle$, $\langle 110 \rangle$, and $\langle 111 \rangle$ directions. Strictly speaking, there is still a tiny long-range contribution from interaction of the moving Ti^{4+} with its replicas three unit cells away. However, because long-range contributions have mainly a dipole–dipole nature,^{9,31,32} which decays with the distance between dipoles, R_D , as R_D^{-3} , it can reasonably be expected that cooperative effects in the $3 \times 3 \times 3$ supercell are negligible compared with those of the $1 \times 1 \times 1$ supercell (about ~ 27 times smaller).

After the local contributions are obtained through this practical procedure, the cooperative contributions are immediately obtained by subtracting the energies of step 1 from those of step 2. We have first carried out this process at ambient pressure using the experimental lattice parameter of BaTiO_3 in its cubic phase.⁶¹ Further on, we have repeated the same kind of analysis, slightly varying the lattice parameter.

Figure 4 shows the main results from the BaTiO_3 study using Slater's model. Let us first consider the results obtained on a $1 \times 1 \times 1$ supercell where all Ti^{4+} ions are equivalent and move in the same way. It can be seen in Figure 4a that, although Ti^{4+} ion off-center displacements are energetically favorable in all of the studied directions, the most stable situation corresponds to motion along the $\langle 111 \rangle$ direction. This situation is thus similar to that found for MnCl_6^{5-} complexes in KCl. It should be recalled, however, that in the present calculations only Ti^{4+} ions are allowed to move,⁶² while for $\text{KCl}:\text{Mn}^+$ a simultaneous movement of the Cl^- ions was indispensable in order to have an off-center displacement. Accordingly, the calculated stabilization energies in BaTiO_3 (Figures 1 and 4) are found to be 5 times higher than those observed for Mn^+ in $\text{KCl}:\text{Mn}^+$.

Nevertheless, the results gathered in Figure 4 point out that, if in a $3 \times 3 \times 3$ supercell we try to move only one Ti^{4+} ion along $\langle 111 \rangle$ at ambient pressure, the off-center motion in the corresponding TiO_6^{8-} complex is not energetically favorable. Thus, a single Ti^{4+} ion in BaTiO_3 is found not to move off-center, contrary to what happens for a Mn^+ impurity in KCl. This fact stresses that the cooperative motion of all Ti^{4+} ions plays a key role for making the ferroelectric distortion at ambient pressure possible, a conclusion that concurs with the results by Junquera and Ghosez¹⁵ showing that in thin films of

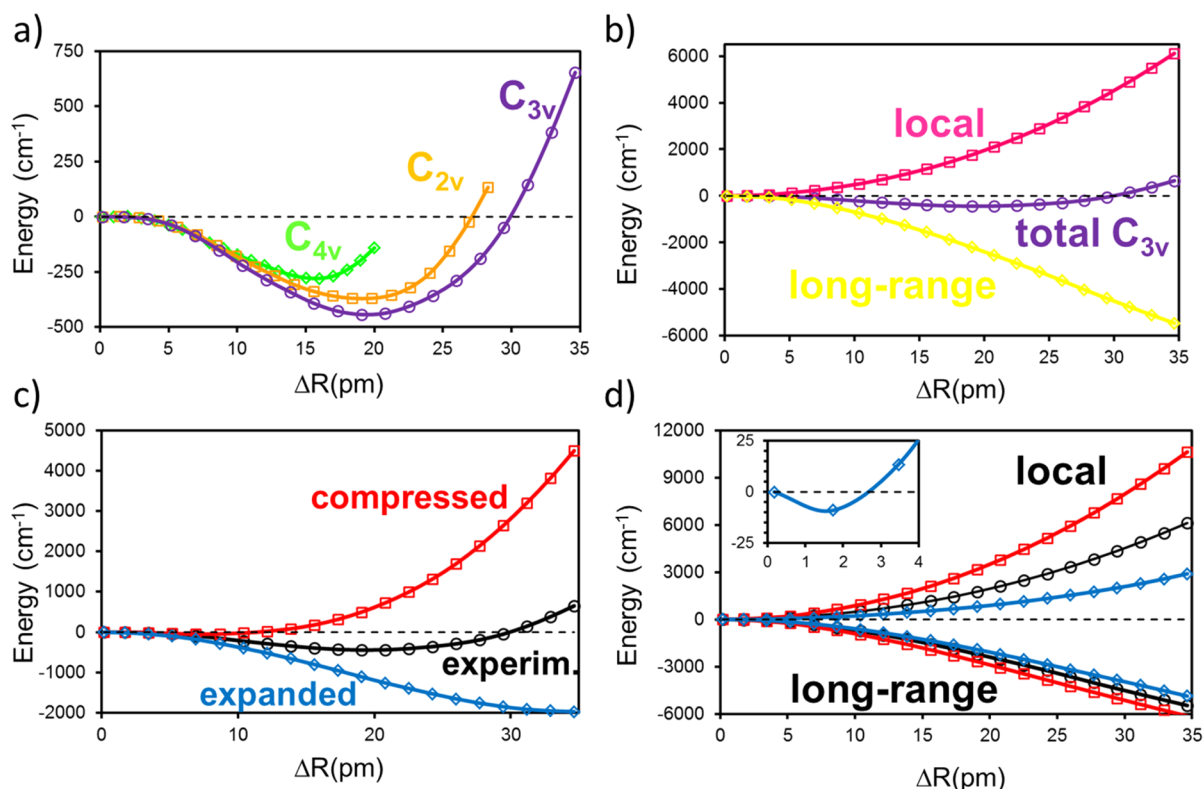


Figure 4. (a) Stabilization energies of BaTiO₃ upon off-center displacements of Ti⁴⁺ ions in the C_{4v} ⟨100⟩, C_{2v} ⟨110⟩, and C_{3v} ⟨111⟩ directions obtained in 1 × 1 × 1 supercell calculations (step 1 in the text) using the experimental lattice parameter of BaTiO₃. (b) Decomposition of the total C_{3v} ⟨111⟩ curve from part a in its local and long-range contributions at ambient pressure. Similar features were also found in the ⟨100⟩ and ⟨110⟩ directions. (c) Stabilization energy of BaTiO₃ upon off-center displacements of Ti⁴⁺ ions in a C_{3v} ⟨111⟩ direction using the experimental lattice parameter and also a unit cell isotropically expanded or compressed 5%. (d) Decomposition of the C_{3v} ⟨111⟩ curves from part c in the local (upper curves in the figure) and long-range (bottom curves in the figure) contributions. The labeling is the same as that of part c. The inset figure shows the local contributions at small displacements for the 5% expanded lattice, revealing the existence of a minimum.

BaTiO₃ there is a critical thickness below which the spontaneous polarization disappears. Nevertheless, this fact does not mean that the existence of ferroelectricity in BaTiO₃ can be understood considering *only* the long-range cooperative interactions. Indeed, the long-range interactions are higher in both CaTiO₃ and SrTiO₃ compounds displaying a *smaller* lattice parameter than that in BaTiO₃, and thus these materials should also be ferroelectric if this phenomenon essentially depends on the cooperative interactions. Therefore, the absence of ferroelectricity in both CaTiO₃ and SrTiO₃ highlights the key role played by the local component for the appearance of a spontaneous polarization. As discussed in section 3.5, the local component is extremely sensitive to variations of the lattice parameter, hindering off-center distortions when it is reduced. This is the reason why there is an off-center motion for KCl:Mn³⁺³³ but not for NaCl:Mn³⁺⁵¹

It could be argued that, if the off-center motion in a single TiO₆⁸⁻ complex is not favored, it can be due to either long- or short-range interactions. In order to check this possibility, we have calculated the electrostatic potential, V_R(r), exerted by the rest of the lattice ions on the complex. The form of eV_R(r) has been calculated for different lattices, and in the case of the cubic perovskite, that quantity is completely flat in the region r < 1.0 Å for different crystallographic directions, as shown in Figure 5. Why V_R(r) is so flat for the normal perovskite structure but not for the inverted one is a matter discussed in ref 63. Thus, according to Figure 5, the long-range electrostatic contributions due to the rest of the lattice ions on a TiO₆⁸⁻ complex do not

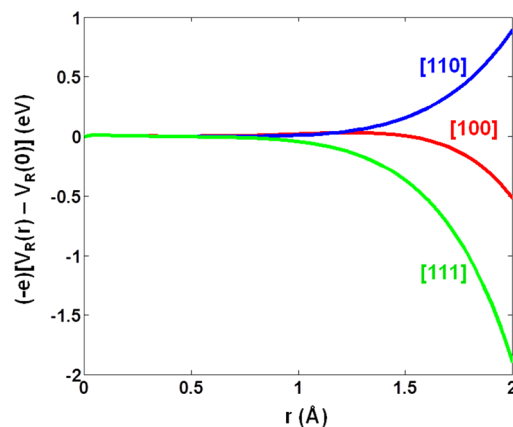


Figure 5. Potential energy, $e[V_R(r) - V_R(0)]$, experienced by a +e charge confined in an octahedral TiO₆⁸⁻ complex due to the electrostatic potential, V_R(r), produced by the rest of the ions of the undistorted BaTiO₃ perovskite lattice depicted along the [100], [110], and [111] crystalline directions.

seem to be a major factor preventing a single Ti⁴⁺ ion to displace off-center in BaTiO₃. As a consequence of these results, the problem of the displacement of a single Ti⁴⁺ ion can be seen as essentially local, where the local pseudo-Jahn–Teller interaction²⁴ favoring distortion is overcompensated by short-range ion–ion repulsions. A quantitative analysis on this issue is given in the next section.

3.5. Link between the Local Contribution to the Ferroelectric Distortions in BaTiO₃ and the Covalent Driving Force of the Off-Center Instabilities in KCl:Mn⁺.

The present results show that at ambient pressure a *single* Ti⁴⁺ ion in BaTiO₃ is not allowed to move off-center. This fact is in contrast with the spontaneous off-center motion for an isolated Mn⁺ impurity in KCl and underlines the importance of the cooperative motion of all Ti⁴⁺ ions in the ferroelectric distortion taking place in BaTiO₃.

Despite the present results at ambient pressure seeming thus to lead to opposite conclusions for KCl:Mn⁺ and BaTiO₃ (i.e., in KCl:Mn⁺, local effects are responsible for the stabilization, whereas in BaTiO₃, they hinder it), the two systems are, however, closer to each other than they appear. We can see this by slightly and isotropically expanding and compressing the BaTiO₃ lattice and looking at the evolution of the local and cooperative contributions. Figure 4c shows that expanding the BaTiO₃ lattice substantially enhances the off-center displacements. On the contrary, we notice that a 5% compression suppresses the effect completely, while in KCl:Mn⁺, the suppression of the off-center instability is reached by reducing *only* 1% of the host lattice parameter. This situation is thus fully similar to that found for Cu²⁺ impurities in CaF₂, SrF₂, and SrCl₂, where an increase of hydrostatic or chemical pressures acts against the off-center motion of the impurity.^{26,27,46}

As a salient feature, Figure 4d also reveals that the local effects in BaTiO₃ are much more sensitive to the change in the lattice parameter than the cooperative ones and control the appearance of ferroelectricity. In fact, on passing from 5% expansion to 5% compression, local effects act progressively against the distortion being enhanced by a factor of ~4. By contrast, the cooperative effects favoring the distortion increase *only* by a factor of ~1.3.⁶⁴ Therefore, cooperative effects can be considered, in a first approximation, constant upon hydrostatic or chemical pressures like in the XTiO₃ (X = Ca²⁺, Sr²⁺, Ba²⁺) series. Thus, Figure 4d stresses that the variation of the local component is the key ingredient behind the existence or disappearance of the off-center instability in ferroelectrics due to pressure changes. These changes directly control the elastic constraints the environment (the rest of the lattice) creates over distortion of a single complex. It is worth noting now that, if we look in detail at the local component for the 5% expanded BaTiO₃ lattice (see the inset in Figure 4d), we notice that a small off-center displacement is already stable. So, our calculations show that local interactions can trigger a spontaneous polarization of the crystal by themselves upon a small increase of the lattice parameter. Thus, while cooperative interactions slowly decrease along the series XTiO₃ (X = Ca²⁺, Sr²⁺, Ba²⁺), the local component of the distortion is very sensitive to changes of the lattice parameter or the chemical environment and is the determining factor to find instability. This situation is completely analogous to what happens in KCl:Mn⁺ where the off-center distortion is destroyed either under a small hydrostatic compression or through changes in the host crystal by NaCl, which has a smaller lattice parameter and is harder than KCl.⁵¹ This fact highlights the importance of properly understanding the microscopic nature of the local effects involving subtle changes in chemical bonding^{26,28,40} as stressed in, for example, the vibronic theory for ferroelectricity.⁶⁵ Therefore, this situation becomes rather similar to that found for KCl:Mn⁺ at ambient pressure, where local changes of the electronic density induced by the distortion favor the off-center displacement, making $K < 0$. Moreover, if the host lattice

is compressed *only* by 1%, that mechanism is against distortion in KCl:Mn⁺ ($K = K_0 + K_v > 0$) similarly to what is found for the local component in BaTiO₃ at ambient pressure (Figure 4b).

Seeking to quantify the results embodied in Figure 4 for BaTiO₃, we can write the total force constant, K , derived from the present calculations as follows:

$$K = K_L + K_C \quad (3)$$

Here, the first component, K_L , corresponds to the local contribution obtained in a $3 \times 3 \times 3$ supercell calculation, while K_C depicts the cooperative component derived through a comparison of the results obtained on $1 \times 1 \times 1$ and $3 \times 3 \times 3$ supercells. Calculated values of K_L and K_C for BaTiO₃ at ambient pressure and under a 5% expansion of the lattice parameter are both given in Table 1. These results stress that

Table 1. Values (in eV/Å²) of Local, K_L , and Cooperative, K_C , Contributions to the Total Force Constant, K , Derived from the Present Calculations Performed at the Equilibrium Lattice Parameter at Ambient Pressure of BaTiO₃ as Well as under a 5% Expansion of the Lattice

	ambient pressure	5% expansion
K_L	11.5	-0.19
K_C	-12.2	-9.86
K	-0.7	-10.05

the total force constant calculated at ambient pressure, $K = -0.7$ eV/Å², obeys nearly to a cancellation of the negative cooperative component, $K_C = -12.2$ eV/Å², by the positive local contribution, $K_L = 11.5$ eV/Å². This situation is, however, strongly modified when looking at the lattice under only a 5% expansion, where the cooperative distortion is slightly reduced to $K_C = -9.86$ eV/Å² but the instability is strongly favored ($K = -10.05$ eV/Å²). These results thus prove not only that the local effects can induce distortion by themselves ($K_L = -0.19$ eV/Å²) but that they are the active factor deciding the presence of distortion in the system when the lattice parameter is slightly varied.

It is important to stress here that in the present practical approach the local and cooperative contributions to the force constant, K , are different than the so-called short- and long-range (dipole–dipole) contributions calculated by Ghosez et al.^{14,66,67} In fact, in the present work, the calculated magnitude of *both* K_L and K_C contributions for the ferroelectric mode is on the order of the typical force constant in an oxide, while in the works by Ghosez et al.,^{14,66,67} the value of the two considered contributions is between 1 and 2 orders of magnitude larger. Thus, the present practical approach shows that the cooperative contribution is not so large as to fully determine the instability. In fact, the strong sensitivity of local contributions to external conditions clearly indicates that it controls the appearance of local dipoles in impurity centers or how ferroelectricity is favored along the series ATiO₃ (A = Ca²⁺, Sr²⁺, Ba²⁺).

Before we end this discussion it should be noticed that, when considering the interaction between dipoles involved in the so-called long-range effects in BaTiO₃, the magnitude of the effective Born charge of a Ti⁴⁺ ion is also related to the chemical bonding *inside* the TiO₆⁸⁻ complex formed by the cation and its nearest anions. This means that local effects inside the TiO₆⁸⁻ unit *enhance* the value of that charge, thus favoring ferroelectric distortion, although the off-center motion of a *single* Ti⁴⁺ ion in BaTiO₃ is not energetically favorable. In

this sense, our results indicate that cooperative interactions favor distortion while local interactions are strongly dependent on external factors like pressure and can be brought to favor the instability or prevent it. What seems clear is that local interactions, which can be directly compared to molecular situations, themselves contain terms that oppose distortion and others that strongly depend on the electronic configuration, which facilitate it, as expressed by the pseudo-Jahn–Teller theory ($K = K_0 + K_v$). Usually these terms are very large (much larger than the cooperative terms calculated here)⁶⁸ and are very sensitive to the chemical nature. This fact, in addition to the similarity between impurity centers like KCl:Mn^+ and pure materials such as BaTiO_3 , seems to indicate that local terms are vital to understanding any off-center movement.

4. CONCLUSION

In summary, it has been shown that at ambient pressure a *single* Ti^{4+} ion in BaTiO_3 is not allowed to move off-center, in contrast to what is found for an isolated Mn^+ impurity in KCl . However, this only means that cooperative interactions are a necessary ingredient for the appearance of a spontaneous polarization in BaTiO_3 , not the origin of the distortion. The latter probably resides in the local component because our calculations show that it is much more sensitive than the cooperative component to pressure variations that control the elastic constraints that the lattice exerts over the complex distortions. Accordingly, such a component *alone* is found to favor the off-center distortion for a $\sim 5\%$ lattice expansion, a situation that is thus similar to that found for the impurity system KCl:Mn^+ at ambient pressure, where the off-center distortion is found to be suppressed only by a 1% reduction of the host lattice parameter. Thus, local interactions are found to be critically sensitive to perturbations either physical (pressure) or chemical (ion substitutions in the lattice) and determine why only BaTiO_3 is ferroelectric in the series XTiO_3 ($X = \text{Ca}^{2+}, \text{Sr}^{2+}, \text{Ba}^{2+}$), although cooperative interactions are similar for all of these lattices. In this regard, we would like to note that the “origin” of a phenomenon cannot be found simply by determining a property (i.e., long-range interactions) that favors its appearance but deciding the factor that significantly changes from system to system and prevents observation of the effect in other compounds.

It is worth noting now that, in cases where an instability takes place in molecules either free or trapped in solids, such a phenomenon has been shown to arise *mainly* from the vibronic mixing of a *few valence* orbitals under distortion.^{40,69} For example, the pyramidalization associated with the off-center motion of the central atom in XH_3 molecules ($X = \text{B}, \text{N}$) is fully dependent on the shape and occupation of the frontier orbitals, as was recently shown with rigorous *ab initio* calculations.⁶⁹

We note here that local contributions are found to be dominant in the case of many other instabilities in cubic perovskites, like the octahedra rotation taking place in KMnF_3 and KFeF_3 ,^{51,70} and are certainly fundamental to understanding the changes in the ferroelectric modes with magnetism.⁷¹

Aside from explaining the surprising LPTs observed in KCl:Mn^+ , the present work emphasizes the deep relationship between the structural phase transitions in ferroelectric materials and LPTs displayed by transition-metal impurities in insulators and the need to understand how the change in the local bonding patterns influences the energy surfaces in these

systems. Further work on structural instabilities in pure and doped solids is currently underway.

■ ASSOCIATED CONTENT

📄 Supporting Information

We provide details on the results and interpretation of the vibrational-level calculations for KCl:Mn^+ . This material is available free of charge via the Internet at <http://pubs.acs.org>.

■ AUTHOR INFORMATION

Corresponding Author

*E-mail: jmgla@dtu.dk.

Notes

The authors declare no competing financial interest.

■ ACKNOWLEDGMENTS

Support by the Spanish Ministry of Economy and Competitiveness under Projects FIS2012-30996 and FIS2009-07083 is acknowledged. J.M.G.-L. acknowledges support from the same source under Project FIS2010-21282-C02-01. Thanks are also due to M. T. Barriuso for critical reading of the manuscript.

■ REFERENCES

- (1) Lines, M. E.; Glass, A. M. *Principles and Applications of Ferroelectrics and Related Materials*; Clarendon Press: Oxford, U.K., 1977.
- (2) Uchino, K. *Piezoelectric Actuators and Ultrasonic Motors*; Kluwer Academic: Boston, 1996.
- (3) Akdogan, E. K.; Leonard, M. R.; Safari, A. *Handbook of Low and High Dielectric Constant Materials for Applications*; Academic Press: New York, 1999.
- (4) Scott, J. F. *Ferroelectric Memories*; Springer: Berlin, 2000.
- (5) Waser, R. *Nanoelectronics and Information Technology: Advanced Electronic Materials and Novel Devices*; Wiley-VCH: Weinheim, Germany, 2003.
- (6) Nonnenmann, S. S.; Spanier, J. E. *J. Mater. Sci.* **2009**, *44* (19), 5205–5213.
- (7) Smith, M. B.; Page, K.; Siegrist, T.; Redmond, P. L.; Walter, E. C.; Seshadri, R.; Brus, L. E.; Steigerwald, M. L. *J. Am. Chem. Soc.* **2008**, *130* (22), 6955–6963.
- (8) Utilization of Poly(Ethylene Terephthalate) Plastic and Composition-Modified Barium Titanate Powders in a Matrix That Allows Polarization and the Use of Integrated-Circuit Technologies for the Production of Lightweight Ultrahigh Electrical Energy Storage Units (EESU). US2005028970, <http://patentscope.wipo.int/search/en/WO2006026136>.
- (9) Bruce, A. D. *Adv. Phys.* **1980**, *29* (1), 111–217.
- (10) Bussmann-Holder, A.; Dalal, N. Order/Disorder Versus or with Displacive Dynamics in Ferroelectric Systems. In *Ferro- and Antiferroelectricity: Order/Disorder Versus Displacive*; Dalal, N. S., Bussmann Holder, A., Eds.; Springer: New York, 2007; Vol. 124, pp 1–21.
- (11) Slater, J. C. *Phys. Rev.* **1950**, *78* (6), 748–761.
- (12) Cochran, W. *Phys. Rev. Lett.* **1959**, *3* (9), 412–414.
- (13) Cochran, W. *Adv. Phys.* **1960**, *9* (36), 387–423.
- (14) Ghosez, P.; Gonze, X.; Michenaud, J. P. *Europhys. Lett.* **1996**, *33* (9), 713–718.
- (15) Junquera, J.; Ghosez, P. *Nature* **2003**, *422* (6931), 506–509.
- (16) Scott, J. F.; Dearaujo, C. A. P. *Science* **1989**, *246* (4936), 1400–1405.
- (17) Comes, R.; Lambert, M.; Guinier, A. *Solid State Commun.* **1968**, *6* (10), 715.
- (18) Chaves, A. S.; Barreto, F. C. S.; Nogueira, R. A.; Zeks, B. *Phys. Rev. B* **1976**, *13* (1), 207–212.
- (19) Ravel, B.; Stern, E. A.; Vedrinskii, R. I.; Kraizman, V. *Ferroelectrics* **1998**, *206* (1–4), 407–430.

- (20) Muller, K. A.; Berlinger, W. *Phys. Rev. B* **1986**, *34* (9), 6130–6136.
- (21) Zalar, B.; Laguta, V. V.; Binc, R. *Phys. Rev. Lett.* **2003**, *90* (3).
- (22) Cohen, R. E. *Nature* **1992**, *358* (6382), 136–138.
- (23) Bersuker, I. B. *Phys. Lett.* **1966**, *20* (6), 589–8.
- (24) Bersuker, I. B. *The Jahn–Teller Effect*; Cambridge University Press: Cambridge, U.K., 2006.
- (25) Bersuker, I. B. *Phys. Rev. Lett.* **2012**, *108* (13), 137202.
- (26) Garcia-Fernandez, P.; Trueba, A.; Garcia-Lastra, J. M.; Barriuso, M. T.; Moreno, M.; Aramburu, J. A. *Jahn–Teller Effect: Fundamentals and Implications for Physics and Chemistry*; Springer: Berlin, 2009.
- (27) Fernandez, P. G.; Aramburu, J. A.; Barriuso, M. T.; Moreno, M. *Phys. Rev. B* **2004**, *69* (17).
- (28) Garcia-Fernandez, P.; Aramburu, J. A.; Barriuso, M. T.; Moreno, M. *Phys. Rev. B* **2006**, *73* (18), 184122.
- (29) Harada, J.; Axe, J. D.; Shirane, G. *Phys. Rev. B* **1971**, *4* (1), 155–8.
- (30) Stern, E. A. *Phys. Rev. Lett.* **2004**, *93* (3).
- (31) Zhong, W.; Vanderbilt, D.; Rabe, K. M. *Phys. Rev. B* **1995**, *52* (9), 6301–6312.
- (32) Zhong, W.; Vanderbilt, D.; Rabe, K. M. *Phys. Rev. Lett.* **1994**, *73* (13), 1861–1864.
- (33) Badalyan, A. G.; Baranov, P. G.; Vikhnin, V. S.; Petrosian, M. M.; Khramtsov, V. A. *Zh. Eksp. Teor. Fiz.* **1985**, *88* (4), 1359–1368.
- (34) Kristoffel, N. N. *Fiz. Tverd. Tela* **1986**, *28* (9), 2827–2829.
- (35) Badalyan, A. G.; Baranov, P. G.; Vikhnin, V. S.; Khramtsov, V. A. *JETP Lett.* **1986**, *44* (2), 110–113.
- (36) Soethe, H.; Vetrov, V. A.; Spaeth, J. M. *J. Phys.: Condens. Matter* **1992**, *4* (39), 7927–7936.
- (37) Garcia-Fernandez, P.; Aramburu, J. A.; Barriuso, M. T.; Moreno, M. *J. Chem. Phys.* **2008**, *128* (12).
- (38) Boettcher, F.; Spaeth, J. M. *Phys. Status Solidi B* **1974**, *61* (2), 465–473.
- (39) Riley, M. J.; Hitchman, M. A.; Reinen, D.; Steffen, G. *Inorg. Chem.* **1988**, *27* (11), 1924–1934.
- (40) Garcia-Fernandez, P.; Garcia-Lastra, J. M.; Trueba, A.; Barriuso, M. T.; Aramburu, J. A.; Moreno, M. *Phys. Rev. B* **2012**, *85* (9), 094110.
- (41) QUANTUM ESPRESSO: A Modular and Open-Source Software Project for Quantum Simulations of Materials: Giannozzi, P.; Baroni, S.; Bonini, N.; Calandra, M.; Car, R.; Cavazzoni, C.; Ceresoli, D.; Chiarotti, G. L.; Cococcioni, M.; Dabo, I. *J. Phys.: Condens. Matter* **2009**, *21* (39).
- (42) Perdew, J. P.; Zunger, A. *Phys. Rev. B* **1981**, *23* (10), 5048–5079.
- (43) Fuchs, M.; Scheffler, M. *Comput. Phys. Commun.* **1999**, *119* (1), 67–98.
- (44) Finch, G. I.; Fordham, S. *Proc. Phys. Soc., London* **1936**, *48*, 85–94.
- (45) The displacements of the K^+ ion in the second shell are negligible in comparison with the displacements of the Cl^- ions in the first shell. In the geometry optimizations, Cl^- ions are allowed to move out of the $\langle 100 \rangle$ (or $\langle 010 \rangle$ and $\langle 001 \rangle$) directions. However, these displacements are also negligible.
- (46) Ulanov, V. A.; Krupski, M.; Hoffmann, S. K.; Zaripov, M. M. *J. Phys.: Condens. Matter* **2003**, *15* (7), 1081–1096.
- (47) de Keersgieter, A.; Callens, F.; Baroen, M.; Matthys, P.; Boesman, E. *Phys. Status Solidi B* **1985**, *130* (1), 297–301.
- (48) Badalyan, A. G.; Petrosyan, M. M.; Khramtsov, V. A. *Fiz. Tverd. Tela* **1986**, *28* (8), 2529–2531.
- (49) Barriuso, M. T.; Ortiz-Sevilla, B.; Aramburu, J. A.; Garcia-Fernandez, P.; Garcia-Lastra, J. M.; Moreno, M. *Inorg. Chem.* **2013**, *52* (16), 9338–9348.
- (50) Lebedev, A. I.; Sluchinskaya, I. A.; Demin, V. N.; Munro, I. H. *Phys. Rev. B* **1997**, *55* (22), 14770–14773.
- (51) Garcia-Fernandez, P.; Aramburu, J. A.; Barriuso, M. T.; Moreno, M. *J. Phys. Chem. Lett.* **2010**, *1* (3), 647–651.
- (52) Ikeya, M.; Itoh, N. *J. Phys. Chem. Solids* **1971**, *32* (11), 2569.
- (53) Garcia-Fernandez, P.; Aramburu, J. A.; Barriuso, M. T.; Moreno, M. *J. Phys.: Conf. Ser.* **2010**, *249*, 012033.
- (54) Garcia-Fernandez, P.; Trueba, A.; Barriuso, M. T.; Aramburu, J. A.; Moreno, M. *Phys. Rev. Lett.* **2010**, *104* (3).
- (55) Garcia-Fernandez, P.; Trueba, A.; Barriuso, M. T.; Aramburu, J. A.; Moreno, M. *Vibronic Interactions and the Jahn–Teller Effect*; Springer-Verlag: Heidelberg, Germany, 2012.
- (56) Ham, F. S. *Electron Paramagnetic Resonance*; Plenum: New York, 1972.
- (57) Riley, M. J.; Noble, C. J.; Tregenna-Piggott, P. L. W. *J. Chem. Phys.* **2009**, *130* (10), 104708.
- (58) Ham, F. S. *Phys. Rev. Lett.* **1987**, *58* (7), 725–728.
- (59) Anderson, P. W. *Phys. Rev.* **1958**, *109* (5), 1492–1505.
- (60) Garcia-Fernandez, P.; Garcia-Canales, L.; Garcia-Lastra, J. M.; Junquera, J.; Moreno, M.; Aramburu, J. A. *J. Chem. Phys.* **2008**, *129* (12).
- (61) Megaw, H. D. *Nature* **1945**, *155* (3938), 484–485.
- (62) The O^{2-} ions adjacent to the Ti^{4+} ion were fixed in order to avoid an extra cooperative effect with the neighbor unit cells in the $3 \times 3 \times 3$ supercell calculations, which would hinder the straightforward decomposition of the energies in the local and long-range components.
- (63) Trueba, A.; Garcia-Lastra, J. M.; Barriuso, M. T.; Aramburu, J. A.; Moreno, M. *Phys. Rev. B* **2008**, *78* (7).
- (64) These factors are an average in the range plotted in Figure 4d.
- (65) Bersuker, I. B. *Chem. Rev.* **2013**, *113* (3), 1351–1390.
- (66) Ghosez, P.; Gonze, X.; Michenaud, J. P. *Ferroelectrics* **1994**, *153* (1), 91–96.
- (67) Ghosez, P.; Gonze, X.; Michenaud, J. P. *Ferroelectrics* **1995**, *164* (1), 113–121.
- (68) Bersuker, I. B.; Balabanov, N. B.; Pekker, D.; Boggs, J. E. *J. Chem. Phys.* **2002**, *117* (23), 10478–10486.
- (69) Garcia-Fernandez, P.; Aramburu, J. A.; Moreno, M.; Zlater, M.; Gruden-Pavlovic, M. *J. Chem. Theory Comput.* **2014**, *10* (4), 1824–1833.
- (70) Babel, D.; Tressaud, A. *Inorganic Solid Fluorides*; Academic Press: New York, 1985.
- (71) Garcia-Fernandez, P.; Antonio Aramburu, J.; Moreno, M. *Phys. Rev. B* **2011**, *83* (17), 174406.